

# Flexible Composite of PEEK and Liquid Crystalline Polymer in Presence of Polyphosphazene

T. Rath,<sup>1</sup> S. Kumar,<sup>1</sup> R. N. Mahaling,<sup>1</sup> M. Mukherjee,<sup>1</sup> C. K. Das,<sup>1</sup> K. N. Pandey,<sup>2</sup> A. K. Saxena<sup>2</sup>

<sup>1</sup>Materials Science Centre, Indian Institute of Technology, Kharagpur 721302, India

<sup>2</sup>Defence Materials and Stores Research Development and Establishment, Kanpur 208013, India

Received 20 July 2006; accepted 17 November 2006

DOI 10.1002/app.25934

Published online in Wiley InterScience (www.interscience.wiley.com).

**ABSTRACT:** Binary blends of a reactive ketone based polymer with liquid crystalline polymer (LCPA-950) were studied. The main properties required are flexibility and thermal resistance of material in presence of polyphosphazene, which acts as a compatibilizer. It has been observed that with the addition of LCP the composites showed reduced viscosity during blending and changes in the crystallization of the LCP phase. FTIR study showed that there was a partial interaction between the PEEK and LCP in presence of polyphosphazene. Polyphosphazene is miscible with both PEEK and LCP, which was evident from DMA results. The thermal stability of the composites has been studied by DTA/TGA. The thermal analysis of the blends showed that the degradation process is accelerated by

blending, but with the addition of polyphosphazene the onset temperature of first degradation slightly shifted towards higher side than the PEEK/LCP blend. Measurement of the tensile properties showed an increase in the elongation as well as enhanced modulus and strength. From SEM micrographs of tensile fractured surfaces, it was revealed that there is good adhesion between the matrix and dispersed phase upon addition of polyphosphazene to ketone based polymer (PEEK) with LCP. © 2007 Wiley Periodicals, Inc. *J Appl Polym Sci* 104: 3758–3765, 2007

**Key words:** flexibility; poly(ether ether ketone); liquid crystalline polymer; polyphosphazene; mechanical properties

## INTRODUCTION

The blends of several polymers have become one of the most interesting means to obtain new materials with specific properties rather than synthesis of new polymers.<sup>1,2</sup> Several properties can be combined by blending several polymers. Some of them can be thus improved in comparison with initial products. For question of thermodynamic data the majority of the polymer pairs are immiscible. Two or several phases may always remain present, but a semicompatibility can exist between them and thus create interaction between the various domains coexisting in the blends. The incompatible blends have bad mechanical properties and a coarse morphology. Interactions of high value speciality polymers with technological importance to modify the final properties of the thermoplastic matrix results in materials with a high added value.

These facts justify the rapid advancements in the blending of thermotropic liquid crystalline polymers (TLCP) with engineering thermoplastics.<sup>3–13</sup> The use of TLCPs is particularly interesting, since these advanced materials have been demonstrated to induce specific directional properties, which improve

the applicability of the thermoplastic matrix in specific application where dimensional stability is of importance. The blending of TLCPs with conventional thermoplastics has been shown to reduce the melt viscosity and improve processibility.<sup>3–6,12,14</sup> During processing, the LCP phase may form a fibrillar structure, resulting in the formation of self-reinforced or *in situ* composites.<sup>5,6,14–19</sup>

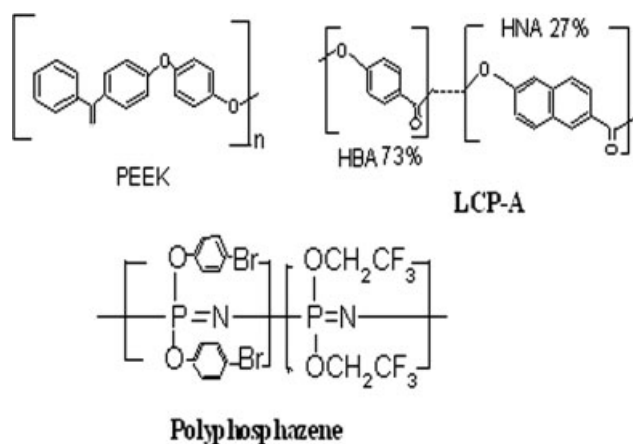
This paper describes the flexible behavior of blends of poly(aryl ether ether ketone) with LCP-A in presence of polyphosphazene, which acts as a compatibilizer. PEEK is a semicrystalline, high performance thermoplastic with  $T_g$  of 143°C and  $T_m$  of 340°C. Its superior mechanical properties and high thermal stability and excellent resistance to hydrolysis have resulted in its extensive usage as structural and load bearing materials in the aerospace and marine industries.<sup>20,21</sup> LCP-A is thermotropic liquid crystalline copolyester with characteristic processing features that impart very high mold flow rates and strength, and has a wide range of applications in the electrical and telecommunications industries.<sup>22,23</sup>

## EXPERIMENTAL

### Materials

The material used in this study was PEEK Poly(ether ether ketone) Victrex 380G supplied by DMSRDE (Kanpur) and thermotropic LCP, VECTRA A950,

Correspondence to: C. K. Das (ckd@matssc.iitkgp.ernet.in).



**Scheme 1** Chemical structural formula of used materials.

based on wholly aromatic copolyester consisting of 73 mol % of *p*-hydroxybenzoic acid (HBA) and 27 mol % 2-hydroxy-6-naphthoic acid (HNA) obtained from Ticona (USA). The compatibilizer used in this study was polyphosphazene (self developed) and the curative used was TMT and ZnO. Chemical structural formula of used materials are shown in Scheme 1.

### Preparation of blends

Before mixing the PEEK and LCP A950 were dried at 80°C for 12 h in a vacuum oven. Blending was carried out in a Brabender plasticorder PL 2200 (mixer N50) equipped with two counter rotating rotor at 340°C and a mixing speed of 60 rpm for 10 min. The procedure was as follows: first the polymer was melted. After that LCP and polyphosphazene were incorporated simultaneously into the molten polymer matrix. Blending formulation is given in Table I. The molded slabs were prepared by compression molding at 340°C for 8 min.

### Fourier transform infrared spectroscopy

Fourier transform infrared spectroscopy (FTIR) experiments were done using a NEXUS 870 FTIR (Thermo Nicolet) in humidity free atmosphere at room temperature. A total of 32 scans were averaged with a resolution of 4 cm<sup>-1</sup>.

### X-ray diffraction analysis (XRD)

X-ray diffraction was studied using a PW-1840 X-ray diffractometer with a Cu K $\alpha$  target at a scanning

rate of 0.05° 2 $\theta$ /s, chart speed of 10 mm/2 $\theta$ , range of 5000 c/s, and a slit of 0.2 mm, applying 40 kV and 20 mA to study the change of the crystallinity of the blends as affected by blend ratio.

The area under the X-ray diffractogram was determined in arbitrary units. The degree of crystallinity,  $X_c$ , and the amorphous content,  $X_a$ , were measured using the following relationship:

$$X_c = I_c / (I_a + I_c) \quad X_a = I_a / (I_a + I_c)$$

where  $I_c$  and  $I_a$  are the integrated intensities corresponding to the crystalline and the amorphous phase, respectively. The crystallite size ( $p$ ) and interplanar distance ( $d$ ) were calculated as follows:

$$P = K\lambda / \beta \cos \theta \quad d = \lambda / 2 \sin \theta$$

where  $\beta$  is half height width (in radian) of the crystallinity peak,  $\lambda$  is the wave length of the X-ray radiation (1.548 for Cu), and  $K$  is the Scherrer constant taken as 0.9.<sup>24,25</sup>

### Thermogravimetric analysis

Thermogravimetric analysis (TGA) and differential-gravimetric (DTG) analysis were carried out using a Dupont TGA-2100 thermal analyzer in the temperature range from 50 to 650°C, with a heating rate of 10°C/min in air.

### Dynamic mechanical analysis (DMA)

Dynamic mechanical thermal properties were determined on a TA instrument DMA 2980 in a single cantilever mode. The samples were subjected to a sinusoidal displacement of 0.1% strain at a frequency of 1 Hz with heating rate 10°C/min. The temperature dependence of storage modulus ( $E'$ ), loss modulus ( $E''$ ), and loss tangent ( $\tan\delta$ ) were measured from 50 to 250°C.

### Mechanical testing

Tensile testing of the blends was done using a HOUNSFIELD (modelH10KS) at constant temperature and humidity. A gauge length of 35 mm and a crosshead speed of 500 mm/min were used. The results reported are the average of four samples for each composite.

### Scanning electron microscope

The morphology of the fractured surface of the specimens was studied by scanning electron microscopy (SEM) after gold coating. A JSM-5800 of JEOL Co. was used at an accelerating voltage of 15 kV.

**TABLE I**  
Sample Codes and Compounding Formulation

Sample No.	L <sub>1</sub>	L <sub>2</sub>	L <sub>3</sub>
PEEK	100	75	75
LCP-A	0	25	22.22
Polyphosphazene	0	0	2.78

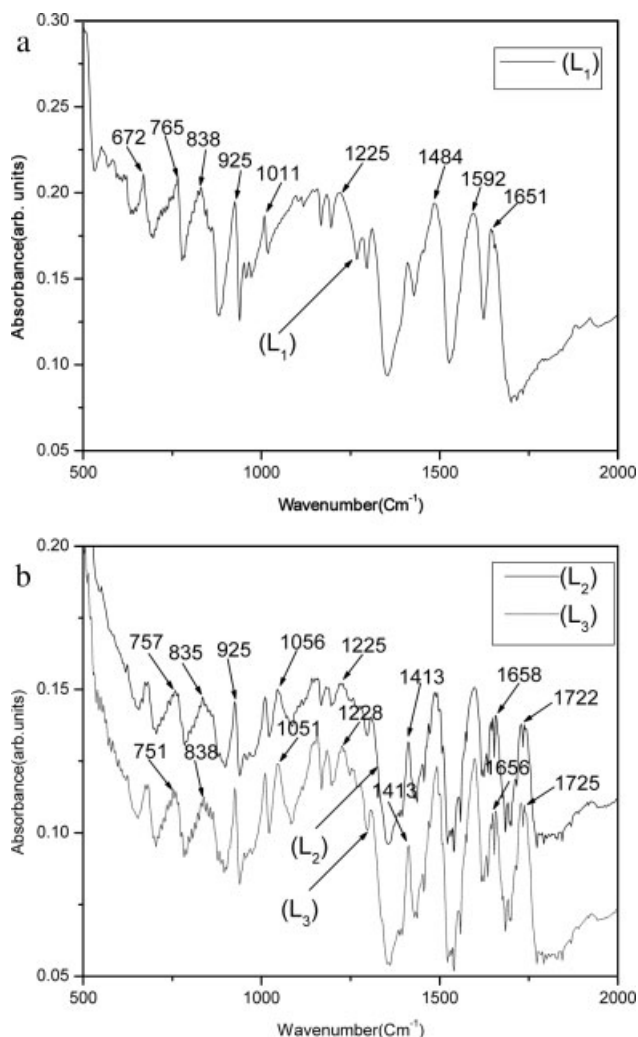


**Figure 1** (a) FTIR spectra of molded thin film of Pure PEEK ( $L_1$ ). (b) FTIR spectra of molded thin film of PEEK/LCP blend ( $L_2$ ) and PEEK/LCP/polyphosphazene blend ( $L_3$ ).

## RESULTS AND DISCUSSION

### FTIR analysis

To study the interaction between PEEK/LCP and PEEK/LCP/Polyphosphazene blends, the FTIR study has been done. The IR spectra of the pure PEEK and the blends are shown in Figure 1. Figure 1(a,b) shows the characteristic bands of pure PEEK and the blends, respectively. Out of all characteristic bands for various groups in the blend, the following peaks are clearly identified:  $1651\text{ cm}^{-1}$  of  $\gamma_{\text{C=O}}$ ,  $1225\text{ cm}^{-1}$  of  $\gamma_{\phi\text{-O-}\phi}$ ,  $1011\text{ cm}^{-1}$  of  $\gamma_{\text{C-O-C}}$  or  $\text{C-O}$ ,  $925\text{ cm}^{-1}$  of  $\gamma_{\text{sy}\phi\text{-(C=O)-}\phi}$ ,  $838$ ,  $765$ , and  $672\text{ cm}^{-1}$  of  $\gamma_{\text{C-H}}$ ,<sup>26</sup> and  $\text{C=O}$  stretching,  $\text{C-O-C}$  symmetry stretching and  $\text{C-O-C}$  asymmetry stretching of LCP appear at  $1733$ ,  $1149$ , and  $1257\text{ cm}^{-1}$  respectively.<sup>27</sup> The assignment of various peaks for the pure PEEK and the LCP are given in Table II. In the blends of PEEK/LCP there is a shift of band at

**TABLE II**  
Assignment of IR Bands of PEEK and LCP-A

Wave number( $\text{cm}^{-1}$ )	Assignment
PEEK	
1,651	C=O stretching
1,225	$\phi\text{-O-}\phi$ stretching
1,011	C-O stretching
925	$\phi\text{-(C=O)-}\phi$ symmetric stretching
838,765,672	C-H stretching
Liquid crystalline polymer	
1,733	C=O stretching
1,149	C-O-C symmetric stretching
1,257	C-O-C asymmetric stretching

$1651\text{--}1658\text{ cm}^{-1}$  and  $\text{C=O}$  of LCP has shifted to  $1722\text{ cm}^{-1}$ , this suggest the probable transesterification reaction at the higher temperature of blending. The change in intensity of the band at  $1225$  and  $925\text{ cm}^{-1}$  of the PEEK is associated with the breakage of ether and ketone linkage to some extent.<sup>28</sup> In presence of polyphosphazene, the band at  $1225\text{ cm}^{-1}$  shifted to  $1228\text{ cm}^{-1}$  and the disappearance of  $\text{C-O-C}$  ( $1011\text{ cm}^{-1}$ ) and the formation of new bands at  $1051\text{ cm}^{-1}$ , suggesting the involvement of polyphosphazene to break of ether and ketone linkage of the PEEK through the nitrogen in polyphosphazene. This has been substantiated by the shifting  $\text{C-Br}$  band of polyphosphazene  $790\text{--}751\text{ cm}^{-1}$ . Again in the presence of polyphosphazene the ester carbonyl stretching has been shifted to  $1725\text{ cm}^{-1}$  and the changing of  $\text{C-Br}$  band as mentioned earlier, suggesting a probable dipole-dipole interaction between LCP and polyphosphazene. However, there is no evidence in the formation of new bonds.

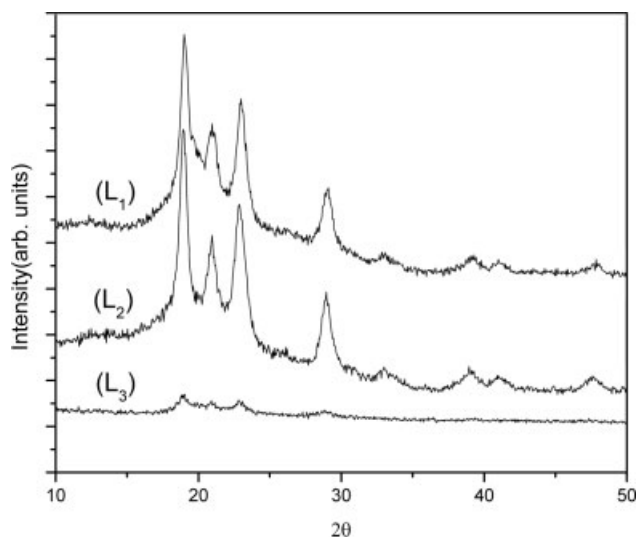


**Figure 2** X-ray diffraction of pure PEEK ( $L_1$ ), PEEK/LCP blend ( $L_2$ ), and PEEK/LCP/polyphosphazene blend ( $L_3$ ).

TABLE III  
X-ray Parameters of PEEK ( $L_1$ ), PEEK/LCP ( $L_2$ ), PEEK/LCP/Polyphosphazene Blends ( $L_3$ )

Sample code	Crystallinity (%)	Inter-planar distance ( $\text{\AA}$ )				Crystallite size ( $\text{\AA}$ )			
		$d_1$	$d_2$	$d_3$	$d_4$	$P_1$	$P_2$	$P_3$	$P_4$
$L_1$	42	4.42	4.25	3.90	3.09	201	125	166	127
$L_2$	53	4.85	4.39	3.97	3.08	213	127	183	133
$L_3$	31	4.15	3.83	3.15	2.87	183	107	143	113

### Wide-angle X-ray diffraction (WAXD) measurement

The WAXD experiment was performed on samples of the PEEK and the PEEK/LCP blends in presence and absence of compatibilizer and the diffractograms are shown in Figure 2. From Figure 2 it is observed that the diffraction pattern of the PEEK and the PEEK/LCP blend appears to be similar, where as a slight increase in intensity is observed for the PEEK/LCP blends. The binary blend with 15% LCP shows an increase in intensity at about  $2\theta = 19^\circ$ , while other peaks corresponding to the PEEK remain unchanged in their peak position and intensity. But in the case of ternary blends, the peaks at about  $2\theta = 19.05^\circ$  and  $22.8^\circ$  shows a significant decrease in the peak intensity with addition of polyphosphazene, indicating that polyphosphazene significantly affect the ordered structure of PEEK by reacting at the interface between LCP and PEEK by forming graft copolymers. The percentage of crystallinity of the blends is increased by the addition of LCP (Table III), but a decrease in crystallinity is observed in presence of polyphosphazene. The increase in crystallinity associated with the increase in crystallite size indicates that LCP acts as a nucleating agent for PEEK/LCP system. In presence of polyphosphazene the PEEK/LCP blend shows lower crystallinity than other systems. This kind of behavior reflects the plasticization effect of polyphosphazene on PEEK and LCP blends. As it was known the compatibilized blends show always lower crystallinity than those of the uncompatibilized derivatives due to the random structure of the formed graft/block copolymers, which will modify the ordered structure of base polymer. Hence, the crystallinity of the blends decreases by the addition of compatibilizer.

### Thermal analysis

The results of the thermogravimetric study of the blends are shown in Figure 3(a,b), respectively, and thermal parameters are summarized in Table IV. The pure PEEK exhibits an initial degradation temperature around  $475^\circ\text{C}$  accompanied by 72% degradation, whereas LCP has an initial degradation temperature of about  $415^\circ\text{C}$ . In case of binary and ternary blend system, the degradation mainly occurs in two steps. For PEEK/LCP system (sample  $L_2$ ), the degradation starts

at  $393^\circ\text{C}$  and continues up to  $502^\circ\text{C}$  at a faster rate and almost 57% of the sample is degraded in this step. The second degradation step starts at  $502^\circ\text{C}$  and found to proceed at a slower rate. Table IV shows that the degradation temperature of PEEK is shifted towards the lower temperature side with addition of LCP. It can be confirmed from the derivative weight loss curves [Fig. 3(b)] that there is a major weight loss at  $546^\circ\text{C}$  for

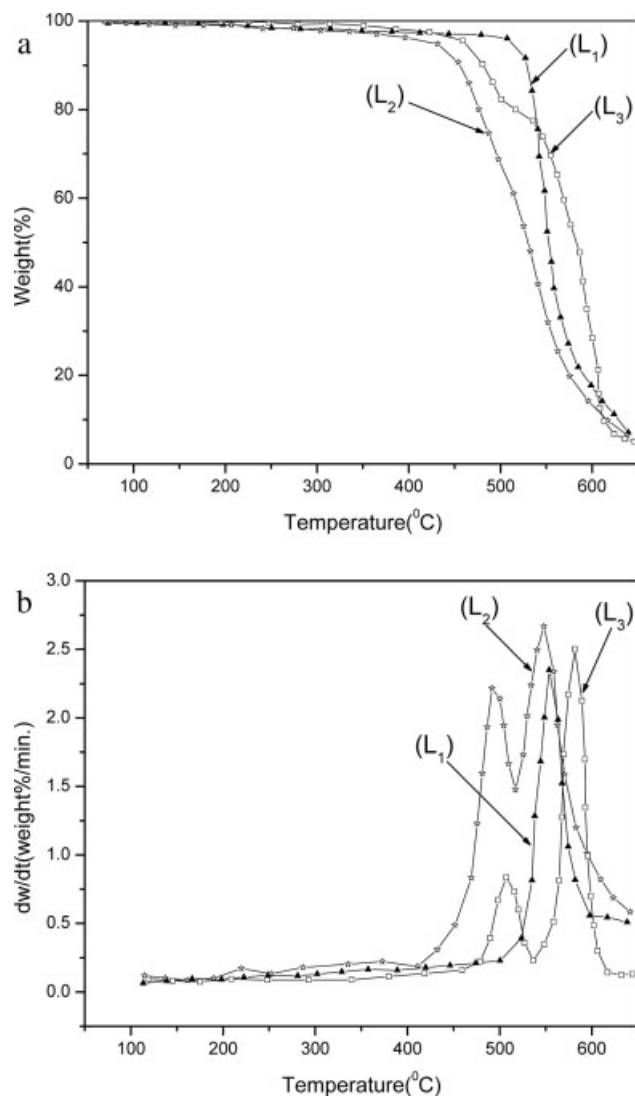


Figure 3 (a) TG analysis of pure PEEK ( $L_1$ ), PEEK/LCP blend ( $L_2$ ), and PEEK/LCP/Polyphosphazene ( $L_3$ ). (b) DTG study of pure PEEK ( $L_1$ ), PEEK/LCP blend ( $L_2$ ), and PEEK/LCP/Polyphosphazene ( $L_3$ ).

**TABLE IV**  
**Thermal Parameters of PEEK ( $L_1$ ), PEEK/LCP ( $L_2$ ), PEEK/LCP/Polyphosphazene Blends ( $L_3$ )**

Sample	First decomposition temperature (°C)	Loss of weight for first step (%)	Second decomposition temperature (°C)	Loss of weight for second step (%)	DTG (°C)
$L_1$	475	72	–	–	546
$L_2$	393	57	502	38	531
$L_3$	428	31	512	48	561

the PEEK, but it is slightly shifted towards the lower temperature side by blending with the LCP; this means that the presence of LCP influences the degradation behavior of PEEK. But in the case of ternary blend system the initial degradation starts at a higher temperature (about 428°C, 512°C) than  $L_2$ . This first degradation process is slower than that for pure PEEK and is associated with 31 and 48% sample degradation, respectively. It can be assumed from the DTG

curves [Fig. 3(b)] that there is a major weight loss at 561°C, which is higher than the PEEK/LCP blend. The higher thermal stability in case of ternary blend system is due to their chemical grafting by polyphosphazene.

### Dynamic mechanical analysis

Loss tangent ( $\tan\delta$ ) of the various blends as a function of temperature is shown in Figure 4 (a). From

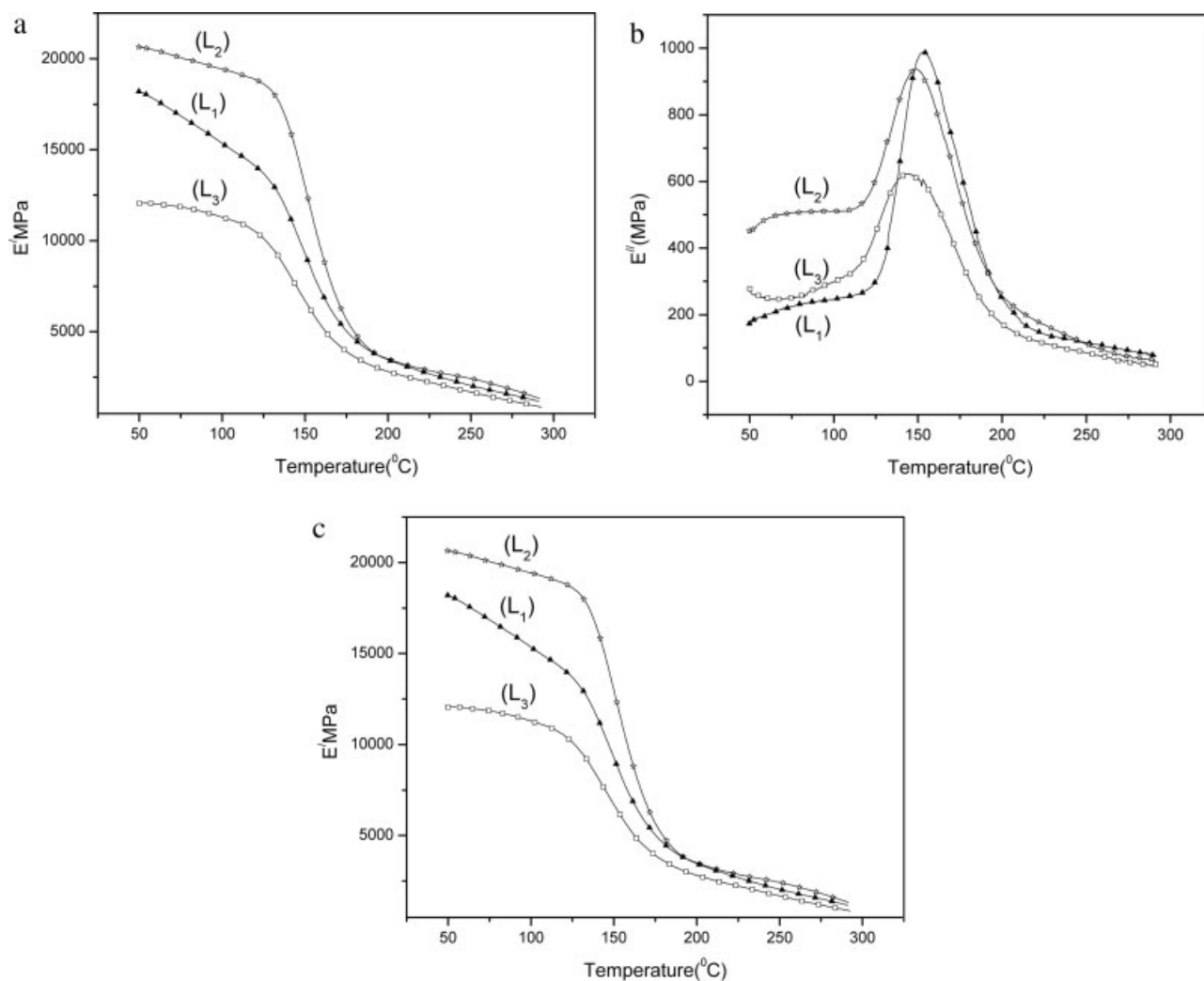


**Figure 4** (a)  $\tan\delta$  as a function of temperature at 1 Hz of pure PEEK ( $L_1$ ), PEEK/LCP blend ( $L_2$ ), and PEEK/LCP/polyphosphazene blend ( $L_3$ ). (b) Loss modulus as a function of temperature at 1 Hz of pure PEEK ( $L_1$ ), PEEK/LCP blend ( $L_2$ ), and PEEK/LCP/polyphosphazene ( $L_3$ ). (c) Storage modulus as a function of temperature at 1 Hz of pure PEEK ( $L_1$ ), PEEK/LCP blend ( $L_2$ ), and PEEK/LCP/polyphosphazene ( $L_3$ ).

Figure 4(a) it is observed that for pure PEEK,  $\tan\delta$  shows a maximum at around 151°C. This is believed to be the  $\alpha$  relaxation for PEEK as referred in the literature.<sup>29</sup> At this temperature the storage modulus is found to drop precipitously [Fig 4(c)]. The temperature at which  $\tan\delta$  shows a maximum has been considered to be the glass transition of the material. The glass transition temperature of polymers is closely related to the flexibility of the chains in the sense that a high value of  $T_g$  is generally assumed to be connected with relatively high barriers of bond rotations. These barriers depend not only on the type of bond, but also on the intermolecular constraint and, therefore, on the supramolecular arrangement of the chains. The height of the  $\tan\delta$  peak is found to decrease with the addition of LCP as seen from Figure 4(a). However, the decrease in  $\tan\delta$  is predominant in the case of ternary blends. This extent of reduction in  $\tan\delta$  of PEEK/LCP by the addition of polyphosphazene may be interpreted as progressive immobilization of the polymer chains close to the boundary between two phases when they are grafted to the polyphosphazene phase. So, it can be concluded that the polyphosphazene enhances the interaction between PEEK and LCP.

The loss modulus ( $E''$ ) of the binary and ternary blends as a function of temperature is shown in Figure 4(b). The loss modulus ( $E''$ ) for binary blends is found to increase with the addition of LCP at 50°C. However, the height of loss modulus peak at a temperature where  $\tan\delta$  shows a maximum is found to decrease with the addition of LCP. The relative decrease in the height of  $\tan\delta$  peak and  $E''$  at  $T_g$  is related to increase in the extent of crystallinity in the polymers, since the transition behavior is associated with the local mobility of the polymer chains in the amorphous region to the polymer region. But with the addition of polyphosphazene in PEEK/LCP blends, the height of loss modulus peak is found to decrease as compared to PEEK/LCP blends, and  $T_g$  is slightly shifted to the lower temperature side due to increase in flexibility of molecular chains.

The storage modulus ( $E'$ ) is closely related to the capacity of a material to absorb or return energy attributed to its elastic behavior.<sup>30</sup> Figure 4(c) shows the variation of storage modulus  $E'$  against temperature. It is evident that the magnitude of  $E'$  increased with the incorporation of LCP to the matrix. This is probably due to increase in the stiffness of the matrix with the reinforcing effect imparted by the LCP, which allowed a greater degree of stress transfer at the interface. In all the samples there is an inflection point lying in between the temperature range of 148–155 °C, which corresponds to the glass transition region of the matrix as observed from the plots. The blends without polyphosphazene show an increase in  $E'$  below the glass transition region as compared

TABLE V  
Mechanical Properties of PEEK (L<sub>1</sub>), PEEK/LCP (L<sub>2</sub>),  
PEEK/LCP/Polyphosphazene Blends (L<sub>3</sub>)

Sample	Tensile strength (MPa)	Elongation at break (%)	Tensile modulus (GPa)
L <sub>1</sub>	81.0	34.3	5.9
L <sub>2</sub>	84.2	29.2	7.6
L <sub>3</sub>	85.3	36.5	7.1

with the matrix. This slight increase in  $T_g$  may be due to interactions caused by the presence of LCP, resulting in improved interfacial adhesion between LCP and the matrix, which restricted the mobility of the polymer chains. But polyphosphazene treated blends shows almost twofold decrease in  $E'$  over the entire range of temperature, i.e., from 50 to 100 °C in comparison to the PEEK matrix. This behavior is attributed to the free volume and the chain mobility of the polymer matrix in presence of polyphosphazene, which leads to ineffective interface and thereby decreasing the magnitude of storage modulus.

### Mechanical properties

Mechanical properties of blends along with the matrix polymer are given in Table V. The composites show higher tensile strength and lower elongation at break compared to the matrix polymer. The increase in strength may be due to the development of highly oriented domains of LCP, which is well distributed in PEEK matrix. Later, this is revealed by fractured surface studies presented below. In certain cases, the mechanical properties are even greater at certain blend composition than the corresponding properties of either polymer in the unblended state. Specific interaction between blend components causes volume contraction on mixing and a loss in free volume of the blend, leading to a higher modulus and strength value than predicted by the rule of mixing.<sup>31</sup> The variation in the tensile strength and modulus of the blend depends primarily on the degree of orientation and fibrillation of TLCP domain, which is embedded in the matrix of PEEK at the time of processing. For immiscible reinforced composites, the elongation generally decreases while the tensile strength increases.<sup>32</sup> In general, the higher the modulus of the composite, the harder the composite and lower the elongation. But in our composite system this unexpected phenomena of increase in elongation as well as modulus, however, is ascribed to the surfactant role of the compatibilizer. Simultaneous increase of tensile strength (or tensile modulus) and elongation can be explained by improved adhesion between the fibril surface and the matrix in presence of compatibilizer and the micromechanism of fracture in the composites. Fibrous composites can fail during monotonic load-

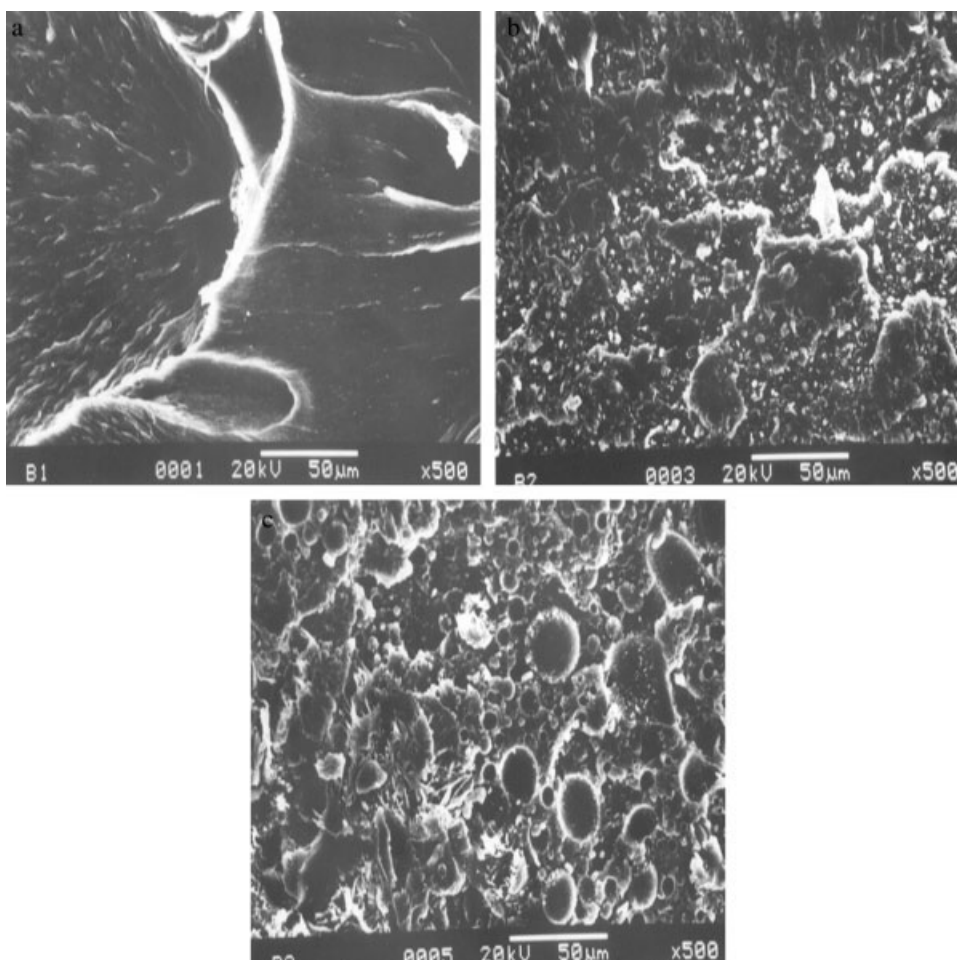


**Figure 5** (a) SEM photographs of fractured surface of pure PEEK ( $L_1$ ). (b) SEM photographs of fractured surface of PEEK/LCP blend ( $L_2$ ). (c) SEM photographs of fractured surface of PEEK/LCP/Polyphosphazene blends ( $L_3$ ).

ing by a number of competing micromechanism of fracture, e.g., by fiber breakage, matrix cracking, and fiber pull-out.<sup>33</sup> Depending on the form in which stored elastic strain energy in the fiber is released, and on the strength and toughness of the fiber, fiber–matrix interface and the matrix, brittle fractures result from the earliest failure event (matrix crack for instance) and the distribution of flaws. A short fiber is pulled out if the force on the fiber is sufficient to cause some debonding. In contrast, for long fibers embedded in a matrix under tensile stress, the fraction of fibers pulled out rather than broken approaches zero as the fiber length increases. This means that such fibers must fracture along a common crack plane or fracture into smaller segments before pulling out of the matrix.<sup>34</sup> When a fiber fractures, in order for the new surfaces to move apart, the matrix must crack or plastically deform and the next fiber must fracture in the crack plane or beyond the crack plane. It is then axially pulled out of the matrix.<sup>33</sup> The matrix plastic deformation and fiber pull-out require additional energy input to the material and provide a means of dissipation of the energy

decrement necessarily associated with fracture. Since the frictional shear force opposes any force applied to extract the fiber, work must be done in overcoming this frictional force. Compatibilized composites have more frictional shear force due to strong adhesion at the interface between the matrix and the fiber, which requires more energy to pull out the fibrils. As a result, the tensile strength (or toughness) of the system increases. Provided the fiber still maintains contact with the sheath of matrix surrounding it, work must be done in pulling the fiber fragments against straining frictional force at the fiber–matrix interface. If the fiber does not maintain contact with the sheath of the matrix, the fibers can be easily pulled out and elongation cannot be increased. However, additional energy should be expended to break strong adhesion at the interface for the compatibilized system. Fibers will not be simply debonded. The fibril is sustained over the gap between crack surfaces until additional energy is supplied. This allows blends containing a small amount of compatibilizer to gain higher elongation at break than non-compatibilized systems.

### SEM study

The homogeneous dispersion of fibers in the polymer matrix is one of the conditions for a composite to show good mechanical strength, because inhomogeneity can lead to structural defects in the composite material. Figure 5 shows the SEM images of the cross-sectional tensile fractured of PEEK, PEEK-LCP, and PEEK/LCP/polyphosphazene blends. The major difference between the binary and ternary blend images are fibrillation of the LCP component in the respective matrix phases. In fact, the mechanical properties of an incompatible blend may depend on enthalpic interaction and related polymer adhesion between phases.<sup>35</sup> Figure 5(b) shows the formation of large voids where the microfibrils were pulled out of the matrix, revealing poor matrix/fibril interfacial adhesion. These micrographs also demonstrate the poor adhesion between the two phases, which leads to an open ring hole around the PEEK matrix and large spherical LCP particles being pulled out during the fracturing of the samples. But in case of ternary blends with the addition of polyphosphazene [Fig. 5(c)], the two matrices are well compatible and better adhesion between the fibers and the polymer matrix of PEEK. It can be visualized from the SEM micrograph that particle size has reduced as particles are entrapped into the matrix. From this observation it is clear that polyphosphazene acts as a compatibilizer for these blends system.

### CONCLUSIONS

*In situ* composites of PEEK/LCP/polyphosphazene were prepared. The miscibility between polyphosphazene and PEEK or Vectra-A was determined by measuring the  $T_g$  shift. Storage modulus of the PEEK matrix decreased with addition of polyphosphazene. The treated blends exhibit a comparatively lower modulus over the entire range of temperature, suggesting that PEEK/LCP blends were flexible in presence of polyphosphazene. An increase in the thermal stability of the polyphosphazene treated blends over the untreated blends was also observed, accompanied by higher decomposition temperature with comparatively less weight loss in the polyphosphazene compatibilized system. FTIR study revealed that partial interaction between PEEK and LCP in presence of compatibilizer. From SEM micrographs of fractured surface, the addition of the compatibilizer to PEEK/LCP blends is found to increase the adhesion between the matrix and the dispersed phase. The compatibilized blends display a much finer dispersion of the minor phase in the matrix

polymer. Polyphosphazene as compatibilizer decreases crystallinity of the triblent system studied.

### References

1. Paul, D. R.; Newman, S. *Polymer Blends*, Vol. 1; Academic Press: New York, 1978.
2. Utracki, L. A. *Polymer Alloys and Blends*; Hanser: New York, 1989.
3. Acierno, D.; La Mantia, F. A., Eds.; *Processing and Properties of Liquid Crystalline Polymers and LCP Blends*; Chem TEC Publishing: Toronto, 1993.
4. La Mantia, F. A. *Thermotropic Liquid Crystal Polymer Blends*; Technomic Publishing: Lancaster, PA, 1993.
5. Kiss, G. *Polym Eng Sci* 1987, 27, 410.
6. La Mantia, F. A.; Valenza, A. *Makromol Chem Macromol Symp* 1990, 38, 183.
7. Blizard, K. G.; Federrici, C.; Federico, O.; Chapoy, L. *Polym Eng Sci* 1990, 30, 1442.
8. Grevecoeur, G.; Groeninckx, G. *Polym Eng Sci* 1990, 30, 532.
9. Isavey, A. L.; Subramanian, P. R. *J Appl Polym Sci* 1991, 32, 85.
10. Mehta, A.; Isavey, A. L. *J Appl Polym Sci* 1991, 31, 963.
11. Subramanian, P. R.; Isavey, A. L. *Polymer* 1991, 32, 1961.
12. La Mantia, F. A.; Valenza, A.; Magagnini, P. L. *J Appl Polym Sci* 1992, 44, 1257.
13. Tjong, S. C.; Liu, S. L.; Li, R. K. Y. *J Mater Sci* 1996, 31, 479.
14. Nobile, M. R.; Acierno, D. *J Appl Polym Sci* 1990, 41, 2723.
15. Blizard, K. G.; Baird, D. G. *Polym Eng Sci* 1987, 2, 653.
16. Weiss, R. A.; Huh, W.; Nicolas, L. *Polym Eng Sci* 1987, 27, 684.
17. Malik, T. M.; Carreau, P. J.; Chapleau, N. *Polym Eng Sci* 1984, 29, 600.
18. Seppala, J.; Heino, M.; Kapanen, C. *J Appl Polym Sci* 1992, 44, 1051.
19. Magagnini, P. L.; Paci, M.; La Manyia, F. A.; Surkova, I. N.; Vasnev, V. A. *J Appl Polym Sci* 1995, 55, 461.
20. Dominghaus, H. *Plastics for Engineers*; Hanser: Munich, 1993.
21. Cogswell, F. N.; *Thermoplastic Aromatic Polymer Composites*; Butterworth Heinemann: Oxford, 1992.
22. Perce, V.; Tomazos, D. In *Comprehensive Polymer Science and Engineering*; Allen, O.; Bevington, J. C., Eds; Pergamon Press: Oxford, 1992; First Supplement, Chapter 2.
23. Weinkauff, D. H.; Paul, D. R. In *Liquid Crystalline Polymers*; Carfagna, C., Ed. Pergmon Press: Oxford, 1994; p 301.
24. Alexander, L. E. *X-ray Diffraction Methods in Polymer Science*; Wiley Interscience: New York, 1969.
25. Rabiej, S.; Ostrowska-Gumkowska, B.; Wlochowicz, A. *Eur Polym J* 1997, 33, 1031.
26. Nguyen, H. X.; Ishida, H. *Polymer Prepr* 1985, 26, 273.
27. Shiva Kumar, E.; Das, C. K.; Pandey, K. N.; Alam, S.; Mathur, G. N.; *Macromol Res* 2005, 13, 81.
28. Naffakh, M.; Ellis, G.; Gomez, M. A.; Marco, C. *Polym Degrad Stab* 1999, 66, 405.
29. Seferis, J. C. *Polym Compos* 1986, 7, 158.
30. Saha, A. K.; Das, S.; Bhatta, D.; Mitra, B. C. *J Appl Polym Sci* 1999, 71, 1505.
31. Sachariades, A.; Porter, P. S., Eds.; *High Modulus Polymer*; Marcel Dekker: New York, 1988.
32. Gent, A. N. In *Science and Technology of Rubber*; Eirich, F., Ed.; Academic Press: New York, 1989; Chapter 10.
33. Beaumont, P. W. R.; Schultz, J. M. *Delaware Composite Design Encyclopedia*, Vol. 4; Technomic: Lancaster, PA, 1990.
34. Harris, B.; Philips, D. C. *J Mater Sci* 1975, 10, 2050.
35. Barlow, J. W.; Paul, D. R. *Polym Eng Sci* 1987, 27, 1482.